Biomass Conversion and Biorefinery
https://doi.org/10.1007/s13399-022-03376-2

ORIGINAL ARTICLE

Bio-oxidization of Mn(II) in acidic wastewater by *Klebsiella* sp. strain M3 and its immobilization towards concomitant Sb(III)

Yongchao Li[1,2] · Jialing Liu[1] · Zhonggeng Mo[2] · Zheng Xu[2]

Received: 23 June 2022 / Revised: 13 September 2022 / Accepted: 9 October 2022

Abstract

Manganese pollution from acid mine drainage has received increasing attention recently. A new strain of acid-resistant manganese-oxidizing bacteria identified as *Klebsiella* sp. strain M3 was isolated and adopted to treat wastewater containing Mn(II) and concomitant Sb(III) in the study. Batch experiment results demonstrated that the strain thrived in an acidic solution, and 36–97.8% of 10 mg/L Mn(II) was removed with inoculation of 2%. Meanwhile, the oxidation activity of the strain was suppressed with the increase of Mn(II) level and decrease of pH, whereas ventilation was beneficial to the Mn(II) removal. The produced dark brown precipitates with high BET surface were composed of poorly crystallized spherical nanoparticles, which were a mixture of FeOOH, MnOOH, and MnO_2. The average Mn oxidation number of manganese oxides was calculated to be 3.63. Moreover, microbial Mn(II) oxidation followed the pseudo-first-order model, and the rate constants were in the range of 0.003–0.024 h^{-1} as the solution pH was between 3.0 and 7.0. The coexistent Sb(III) was removed from the water and immobilized in precipitates along with the biological mineralization of Mn(II). Furthermore, the Sb(III) removal ability of in situ Mn oxides expressed as Sb/Mn mass ratio varied from about 0.15 to 0.7. The results demonstrated that the oxidation capacity of *Klebsiella* sp. strain M3 was strong even in acidic conditions and provided theoretical support for the treatment of large-scale Mn(II)-containing wastewater.

Keywords *Klebsiella* sp. strain M3 · Acidic wastewater · Microbial oxidation · Mn(II) · Sb(III)

1 Introduction

Manganese (Mn) pollution in surface water and groundwater has received increasing attention in recent years [1]. Generally, Mn(II) is the most common oxidation state in water with a pH lower than 7.0, while the more highly oxidized Mn(III, IV) exists at higher pH values and redox potentials. Excessive Mn will not only cause toxicity to the nervous system of humans but also leads to the occurrence of many birth defects [2]. The European Commission and the US Environmental Protection Agency have suggested a guidance value of 0.05 mg/L in drinking water [3, 4]. Furthermore, the most environmentally significant Mn contamination could be directly related to the mining industry, especially in Russia, Brazil, South Africa, and China which host the major manganese ore resources in the world [5–7]. A large amount of wastewater was generated during the process of mining and beneficiation of manganese ore. The pH of wastewater ranged from 3.5 to 6.5, and Mn mainly exists in the form of soluble Mn(II) [8, 9].

Many countries have tried their best to control this non-degradable heavy metal pollution. Up to now, chemical precipitation has been widely used to remove Mn ions from wastewater in the mining industry. Limestone, quartzite dolomite, and magnesite are commonly added to increase effluent pH and alkalinity. However, large amounts of sludge can be produced which need to be treated further [10, 11]. As for adsorption, ion exchange, and chemical oxidation techniques, they are not appropriate for the treatment of manganese mine drainage, due to the high consumption of chemical reagents and energy [12–14].

✉ Yongchao Li
nkliyongchao@163.com

[1] Key Laboratory of Recycling and Eco-Treatment of Waste Biomass of Zhejiang Province, School of Environmental and Natural Resources, Zhejiang University of Science and Technology, Hangzhou 310023, People's Republic of China

[2] School of Civil Engineering, Hunan University of Science and Technology, Xiangtan 411201, People's Republic of China

Published online: 17 October 2022

Since the 1980s, bio-oxidization of Mn(II) has been proven to be a low-cost, high-efficiency method for Mn(II) removal from water at many laboratories and water treatment plants [15–17]. A variety of manganese-oxidizing bacteria (MnOB) that can oxidize Mn(II) and form insoluble biogenic manganese oxides (BMO) were found in natural environments (e.g., soil, water, and sediment). Meanwhile, some fungal strains also played an important role in the removal of heavy metal pollutants [18, 19]. The majority of chemoheterotrophic microorganisms oxidize Mn(II) predominantly via an Mn oxidase enzyme, such as multicopper oxidases (MCOs), lactase, Mn peroxidase, and lignin degradation enzymes [16, 20–25]. Most MnOB are distributed among the genera *Pseudomonas*, *Bacillus*, *Pedomicrobium*, and *Leptothrix* [20, 21]. Literature also indicated that MnOB possessed high oxidation activity over a wide range of Mn levels (< 1 mg/L to > 100 mg/L) and temperatures (4–37 °C) [9, 22]. However, its activity was influenced obviously by water acidity, and the optimal pH value for biological Mn(II) oxidation was in the range of 6.5–8.0 [15–17, 22]. More importantly, cell growth and activity of the Mn oxidase enzyme were seriously inhibited in a highly acidic environment [18, 23, 24]. It was found that when *Pseudomonas putida* strains MnB1 was cultivated in Mn(II) solution with initial pH of 7.5 for 30 h, 10 mg/L of amorphous β-MnO_2 was generated. But, as pH decreased to 5.6, only 2 mg/L of Mn oxides was produced after 40 h of cultivation [20]. More seriously, isolated *Bacillus* sp. T1151 could lose any ability to oxidize Mn(II) if the water pH was lower than 4.0, despite the highest Mn(II) oxidation rate at a pH of 7.0 [25]. Given the lower pH of acid mine drainage and its high Mn(II) content, it can be inferred that Mn(II) oxidation activity in this situation by common MnOB will be very low. Consequently, in the treatment of large-scale acid mine drainage, biological oxidation and removal capacities of Mn(II) would not achieve satisfactory effects. Screening of acid-resistant MnOB with high activity in a specific environment is of great significance for Mn(II) removal from acidic wastewater.

In addition, pyrolusite and rhodochrosite minerals were the most important Mn ore resources, which are usually frequently associated with pyrite and franklinite [26, 27]. Besides Mn, other heavy metals were also found in mine drainage [28]. In special, Sb(III) can coexist with Mn(II) in acidic wastewater as a result of the mining of langbanite, manganostibite, and melanostibite [29]. While raw groundwater used as drinking water sources in China can also be co-contaminated by Mn(II) and Sb(III) [30], it was known that biogenic manganese oxides were excellent adsorbent towards heavy metals, due to the abundant vacancies in their amorphous structure [31, 32]. However, there is not enough study about the simultaneous removal of associated metal in Mn mine drainage during the biological oxidation of Mn(II). What is more, the translocation and transformation of Sb have received less attention compared with other heavy metals, such as Cd, Cu, and As. So, more attention should be paid to the adsorption and speciation of Sb(III) during the treatment of Mn mine wastewater.

In this study, a new strain of acid-resistant MnOB was screened from activated sludge in a sewage treatment plant in Xiangtan city, which was known as "the capital of manganese ore" in China. This study aims to (1) identify and characterize the isolated strain; (2) investigate the biological oxidation and removal behavior of Mn(II) from the solution under different conditions; (3) analyze Mn(II) oxidation kinetics in acidic wastewater by the isolated strain and characteristics of the biogenic product; and (4) reveal the removal mechanism of associated Sb(III) along with the biomineralization process of Mn oxides.

2 Materials and methods

2.1 Isolation of acid-resistant manganese-oxidizing bacteria

The new strain of MnOB was selected from the activated sludge in the aeration tank of Hexi sewage treatment plant in Xiangtan city. The plant can collect wastewater from the nearby manganese mining areas, most of which have been closed for several years, though some are still in production. PYCM and JFM medium with a pH of 5.0 were used for cultivating and isolating MnOB, and the detailed composition of the medium is presented in Table S1. The isolation process was as follows. Fifteen grams of sludge was first added to 90 mL of deionized water. After vibration for 30 min, 5 mL supernate was extracted and added to 150 mL PYCM medium. After the enrichment for 2 days at 30 °C, the formed cell suspension was diluted into four gradient concentrations (10^{-1}, 10^{-2}, 10^{-3}, and 10^{-4}), and spread onto solid media to obtain a single colony. Then, several single colonies were picked up and transferred into JFM medium for 5 days of cultivation. Using the streak plate method, several pure cultures of MnOB were obtained finally through successive isolation.

2.2 A contrast between Mn(II) tolerance in each isolated strain

Investigation of Mn(II) resistance of each isolated strain was conducted as follows. A certain amount of bacteria suspension was evenly spread onto the JFM solid medium with a pH of 5.0, where the gradient of Mn(II) concentration ranged from 0 to 1400 mg/L, separately. After being cultured for 3–5 days, the tolerance of each strain towards Mn(II) was evaluated according to the number of generated colonies. The strain with high tolerance and removal ability

towards Mn(II) under acidic conditions was selected and used further. Meanwhile, leucoberbelin blue I (LBB) which selectively reacted with Mn(III)/Mn(IV) oxides was used for qualitative analysis of manganese oxide formation [33].

2.3 Characterization and identification of the bacterial isolate

The morphological characteristic of the selected strain was studied as follows. First, bacterial suspension was cleaned with 0.1 mol/L phosphate buffer solution and transferred to a 1.5-mL Eppendorf tube. After natural settlement for 1 h, the supernatant was gently discarded. Then, 1 mL of fresh pre-cooled 2.5% glutaraldehyde was slowly added to the tube for fixation. Finally, cell structure characteristics of the strain were observed by transmission electron microscopy (TEM, Tecnai G2 F20 S-Twin, FEI, USA).

The growth characteristic of the isolated strain was investigated in flasks. The strain was first inoculated in 100 mL JFM broth after its pH values were pre-adjusted to 2.0, 3.0, 4.0, 5.0, 6.0, and 7.0, respectively. Then, the cultures were kept on a shaker at a rotational speed of 150 r/min. The aliquots of samples were collected from each flask starting from inoculation, and the optical density (OD) value representing bacteria biomass was measured. After cultivation for 72 h, the suspension was collected and added to 250-mL conical flasks containing 10 mg/L Mn(II) solution.

The strain of MnOB was further identified by phylogenetic analysis. Bacterial genomic DNA of the strain was first extracted [34], and then, PCR amplification of the bacterial V3-V4 region of the 16S rDNA gene was performed using 341F and 805R [35]. After purification of the amplified fragments, it was sequenced by Sangon Biotech (Shanghai) Co., Ltd. The obtained sequenced 16S rDNA gene of the isolated strain was compared with sequences in the GenBank database, and the sequences of eleven closely related type strains were selected. Finally, the 16S rDNA sequences of the isolated strain and the reference strains were used to construct a phylogenetic tree using the software MEGA 7.

2.4 Removal potential of isolated strain towards Mn(II) under different conditions

The removal of Mn(II) from water by obtained MnOB strain was conducted at 30 °C in an incubator. Ten milliliter inoculum of log-phase cells was added to conical flasks containing 490 mL Mn(II) solution, which was covered with a permeable silica gel stopper. During the whole reaction process, no more culture for bacteria growth was added. At timed intervals, residual Mn(II) in water was analyzed. To test the effect of Mn(II) concentration on the oxidation ability of the strain, Mn(II) concentration in acidic water varied from 10 to 50 mg/L. To evaluate the effect of pH on Mn(II) removal ability of isolated strain, the initial pH of Mn(II) solution was pre-adjusted to the desired level from 2.0 to 7.0. In addition, to study the influence of dissolved oxygen on the biological Mn(II) oxidation, the reaction was also conducted in anaerobic bottles.

2.5 Sb removal performance in acidic wastewater along with the microbial Mn(II) oxidation

The isolated strain was first inoculated in conical flasks filled with a mixed solution of Sb(III) and Mn(II) ions. In order to highlight the simultaneous removal of associated metal, we set a higher level for Sb (10 mg/L) in all the flasks, but Mn content was 10, 20, 30, 40, and 50 mg/L, respectively. Moreover, the pH of the mixed solution was pre-adjusted to 3.0, 4.0, 5.0, 6.0, and 7.0, separately. The reaction condition was the same as described above. The concentrations of residual Sb and Mn and colony-forming unit (CFU/mL) were analyzed during the whole reaction process.

2.6 Characterization of bio-generated precipitates and reaction products

The generated dark brown precipitates and Sb removal reaction products were collected and used for characterization. The morphology of the samples was surveyed using scanning electron microscopy (SEM, Zeiss gmini300, Germany). The chemical composition was examined using energy-dispersive X-ray spectroscopy (EDX, Bruker XFlash6I30 Germany) coupled with SEM. Fourier transform infrared spectrometry (FTIR) data were obtained on a Nicolet is50 spectrometer (Thermo Fisher Scientific, USA) using KBr pressed disk technique. The crystallinity and compositions were determined by X-ray diffraction (XRD, D8 Advance, Bruker, Germany) using monochromatized Cu/Ka radiation. The specific surface area was measured by the Brunauer–Emmett–Teller (BET) isotherm using a NOVA2200e surface area and pore size analyzer (Quantachrome Instruments, USA). X-ray photoelectron spectroscopy (XPS) analysis was conducted with an electron energy spectrometer (Escalab 250Xi, Thermo Scientific, USA).

2.7 Analytical methods

Total Sb and Mn in water were analyzed with the flame atomic absorption spectroscopy method [36]. Solution pH and dissolved oxygen concentration were analyzed by a portable dissolved oxygen meter (HQ30D, Hach Company, USA). The OD of bacteria suspension was measured by a UV–vis spectrophotometer at 600 nm. The number of CFUs in the samples was measured by surface plating at appropriate dilutions [37]. All the batch experiments were

conducted in triplicate, and the collected data in our study were expressed as mean ± SD.

3 Results and discussion

3.1 Isolation of MnOB and evaluation of their tolerance towards Mn(II)

After enrichment and isolation in culture, seven strains of MnOB were obtained from sludge, which was named strain M1, M2, M3, M4, M5, M6, and M7, respectively. In order to treat manganese mine drainage, the tolerance of each strain towards Mn(II) was tested under acidic conditions. As can be seen from Table S2, most of the strains grow well in plates where Mn(II) concentration was lower than 200 mg/L. With the increase of Mn(II) concentration, the number of colonies in the medium decreased especially strains M6 and M7. However, strains M2 and M3 were still able to grow up to 1200 mg/L Mn(II), and the other strains could not survive. The different results in Table S2 imply that the strain M3 was tolerant to a high Mn(II) concentration. This was probably because the toxic effect caused by the high Mn(II) level can be reduced to some extent, as a result of the surface adsorption, precipitation extracellular, and intracellular detoxification of living cells [38, 39].

After the strain M3 was inoculated to Mn(II) solution and cultivated for 24 h, 0.04% LBB solution which employed acetic acid as a solvent was added to the mixture. As shown in Fig. S1, different from deionized water, the color of Mn(II)-contained solution becomes dark blue which confirmed the production of manganese oxides [33, 40]. Although solution pH increased to about 6.1 from the initial 5.0, the abiotic oxidation rate of Mn(II) was extremely slow under acidic conditions [13, 41]. LBB was also added to Mn(II) solution without inoculation, and the mixture did not become dark blue, which was similar to that of deionized water. So, the phenomenon of color change proved that the manganese oxides were produced as a result of microbial Mn(II) oxidation in the acidic solution. Given that the acid-resistant strain M3 had the ability to oxidize Mn(II), it was selected for further treatment in the batch experiment.

3.2 Characterization and molecular identification of isolated strain M3

The colonies of isolated strain M3 heaved from the plate JFM medium and exhibited a red-brown metallic luster with a smooth and dry surface. Figure 1a and b are the TEM images of the strain. It can be seen that the strain M3 was typically rod-shaped, and the bacterial size was about 0.5–0.8 × 1.0–2.0 μm. The cells did not have flagella but had cilia. Moreover, bacterial cells secreted some extracellular material in the form of a capsule.

pH is an important environmental factor. It can change the activity of extracellular hydrolase, the permeability of cell membranes, and gene expression, thereby affecting cell growth and activity [42, 43]. Figure 1c is the growth curve of strain M3 under different initial pH. When culture pH was in the range of 5.0–7.0, the growth of strain M3 was in the lag phase during the first 16 h, and then, it grew quickly and reached the stationary phase at approximately 40 h of incubation. As the initial culture pH decreased to 3.0 and 4.0, the lag phase of strain M3 and the reaction period required for the BMO generation were relatively long. However, the strain could not survive at a culture pH of 2.0. Inhibitory effect of the acidic condition also occurred to the growth of other strains of MnOB, such as *Pseudomonas putida* strains MnB1, *Bacillus* species, and *Leptothrix discophora* SS1 [20, 25, 44]. However, even though the nutrient pH was as low as 3.0 or 4.0, the OD of bacteria biomass in our study still reached 0.30 and 0.48, demonstrating that the isolated strain M3 had strong

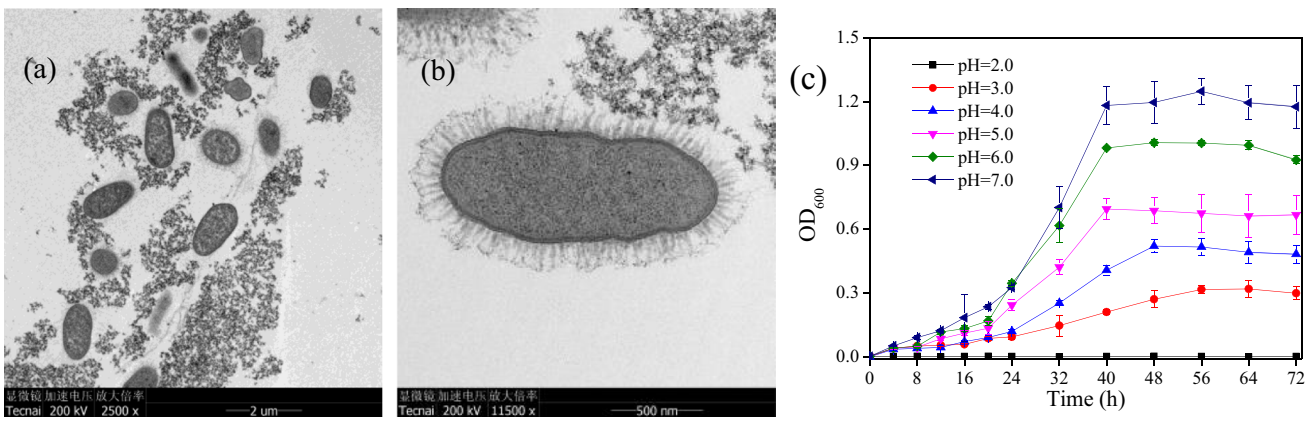

Fig.1 **a** and **b** TEM images of the isolated strain M3 and **c** its growth curves under different pH

acid resistance. Moreover, Mn(II) concentration in the solution decreased from an initial 10 to about 9.7 mg/L, after adding obtained biomass, which may suggest that the isolated strain M3 had weak adsorption ability towards Mn(II).

The 16S rDNA gene sequences of the strain were deposited into the GenBank database with accession No. MW725160. As shown in Fig. 2, the isolated strain M3 belonged to the *Klebsiella* genus, based on the 16S rDNA gene sequencing and phylogenetic analysis. The homology of strain M3 to the nucleotide sequence of *Klebsiella* sp. strain K-21 was 97%; however, they did not belong to the same branch. Now, the isolated *Klebsiella* sp. strain M3 has been preserved in China Center for Type Culture Collection (CCTCC), and the preservation number is CCTCC M 2,021,261.

To our knowledge, the *Klebsiella* genus that can oxidize Mn(II) was rarely reported, but it played an important role in wastewater treatment. For example, *Klebsiella* sp. strain TR5, which was isolated from a chicken manure mixture on a large broiler farm, can efficiently detoxify tetracycline in wastewater and generate much fewer toxic products once cultured for more than one day [45]. A strain of *Klebsiella pneumoniae* L17, which was isolated from the subterranean forest sediment in Zhaoqing, China, was found to be capable of Fe(III) reduction in anaerobic environments [46].

3.3 Mn(II) oxidation and removal ability of *Klebsiella* sp. strain M3

3.3.1 Effect of initial Mn(II) concentration

As shown in Fig. 3a, when Mn(II) concentration ranged from 10 to 50 mg/L, its removal behavior from acidic solution by *Klebsiella* sp. strain M3 with the inoculation of 2% had a certain similarity. Residual Mn(II) in water declined as the reaction processed, and the concentration generally leveled off after about 120 h. At initial Mn(II) concentration of 10, 20, 30, 40, and 50 mg/L, the final Mn(II) content in water was 0.45, 3.55, 6.79, 14.6, and 27.68 mg/L, separately. According to the following formula:

$$\text{Removal rate} = \frac{[\text{Mn}^{2+}]_0 - [\text{Mn}^{2+}]_t}{[\text{Mn}^{2+}]_0} \times 100\% \quad (1)$$

where $[Mn^{2+}]_0$ was the initial Mn(II) concentration and $[Mn^{2+}]_t$ was the Mn(II) concentration after time t (hour). The corresponding removal rates were calculated to be 95.5%, 82.2%, 77.4%, 63.5%, and 44.6%, respectively. It can be seen that the Mn(II) removal rate of isolated *Klebsiella* sp. strain M3 was decreased as Mn(II) concentration increased.

3.3.2 Effect of solution pH

Mn(II) removal ability of *Klebsiella* sp. strain M3 was also investigated as water pH was in the range of 2.0–7.0. As shown in Fig. 3b, when initial solution pH was 7.0, 6.0, 5.0, 4.0, and 3.0, the final removal rate of Mn(II) is about 97.8%, 95.5%, 73.3%, 52.2%, and 36%, respectively. Especially, Mn(II) was barely removed under a highly acidic condition (pH 2.0). At the end of the experiment, the suspension pH increased by 0.3–0.8. It was known that Mn(II) was the most stable oxidation state, and it did not take auto-oxidation under acid or neutral conditions [9, 13, 41], and then, the effect of natural oxidation on Mn(II) removal under this condition can be ignored. Plus, the adsorption ability of biomass towards Mn(II) was very weak in this study. So, it can be inferred that Mn(II) removal was mainly due to microbial Mn(II) oxidation and forming precipitates out of water.

It can be seen that the oxidation capacity of strain M3 decreased with the increase of solution acidity. This was probably because the activities of Mn oxidase enzyme, such

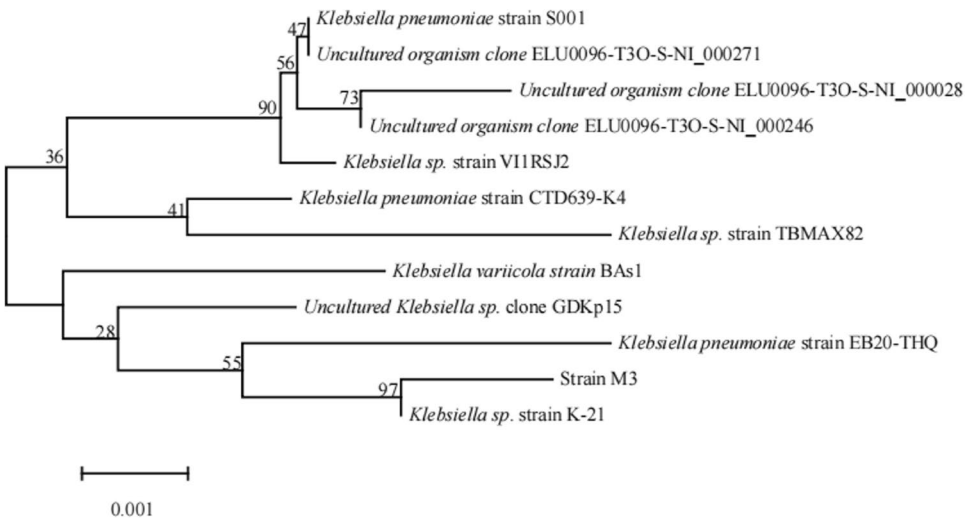

Fig. 2 Phylogenetic tree of the isolated strain M3 based on 16S rDNA gene sequence

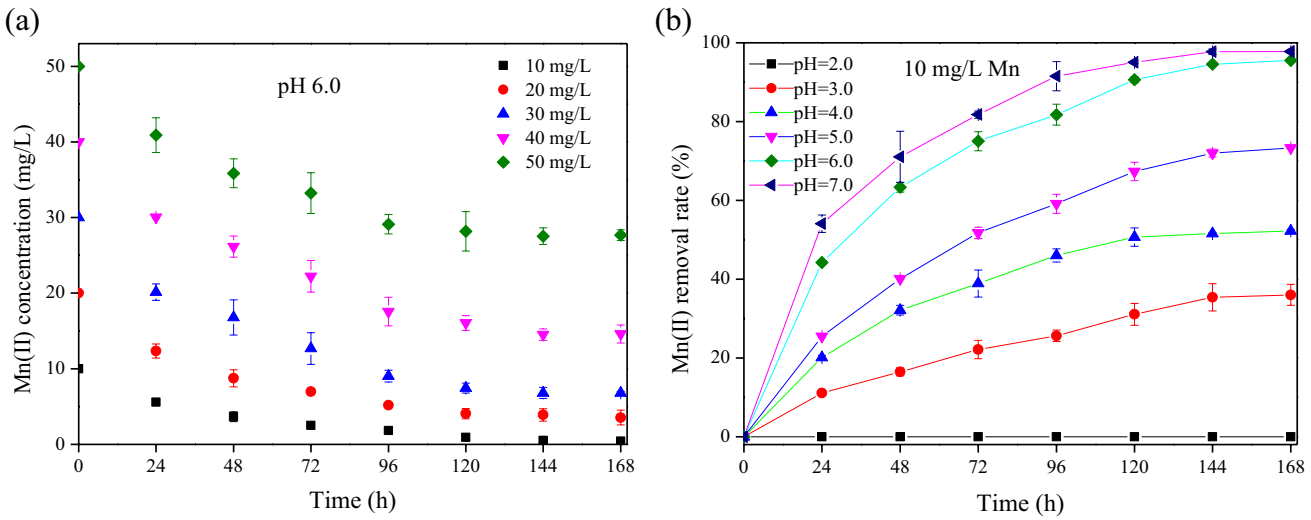

Fig. 3 **a** The change of residual Mn in solution as the reaction process and **b** Mn(II) removal rate of strain M3 under different solution pH

as multicopper oxidase *CueO*, non-blue laccase of *Bacillus* sp. GZB, and purified laccase-like fungal enzymes, were seriously inhibited at acidic pH [23, 24, 40]. However, it is remarkable that bio-oxidation of Mn(II) by *Klebsiella* sp. strain M3 happened even though the solution pH was as low as 3.0. To our knowledge, this was the first time that a strain of MnOB can oxidize Mn(II) in such extreme acidic conditions.

3.3.3 Effect of dissolved oxygen

Mn(II) removal in previous experiments was conducted in ventilated conditions. To study the effect of dissolved oxygen on the activity of strain M3, the reaction is also performed in anaerobic bottles, and the results are shown in Fig. S2a. It demonstrated that Mn(II) removal rate in airtight conditions increased during the first 24 h and then slowed down during the following time. The final removal rate of 10 mg/L Mn(II) by *Klebsiella* sp. strain M3 was 55.2%, which was 40.3% lower than that in ventilated conditions. The change of dissolved oxygen in the solution was not convenient to measure in airtight conditions, but it was measured in ventilation conditions. As shown in Fig. S2b, dissolved oxygen decreases significantly from the initial 11.5 to about 8.0 mg/L at the 6th hour, and then hovers around 7.5 mg/L until the end of the experiment, which was probably because that the subsequent consumption of oxygen by active bacteria and oxygen supply by air diffusion reached a balance. Mandernack et al. applied isotope-labeled oxygen to the oxidation process of Mn(II) by *Bacillus* sp. SG-1 and found that 30 ~ 50% of the oxygen in the manganese oxides product came from oxygen [47]. Thus, to improve the Mn(II) oxidation and removal ability by MnOB, ventilation can be employed in real practice.

3.4 Characterization of biogenic Mn-contained precipitates

Figure 4a shows the SEM image of generated dark brown sediment after bio-oxidation of Mn(II). It was mainly composed of spherical particles, the size of which was about 20 nm. These small particles had a relatively rough surface and agglomerated together to form larger clusters. However, Wan et al. found that the biogenic manganese oxides produced by a manganese-oxidizing bacterial consortium presented irregular shapes of different sizes and loose structures [22]. Its EDX data is shown in Fig. S3, and the presence of elements Fe, Mn, and O is attributed to the formation of manganese oxides and iron oxides. In addition, there were no obvious crystalline peaks on the XRD patterns of the sample (Fig. S4), which indicated that the generated product was poorly crystallized.

Figure 4b shows the FTIR spectra of the sample. Two bands at 3379.4 and 1617.5 cm^{-1} were attributed to O–H stretching vibration and bending vibrations of adsorbed H_2O molecules [48]. The band centered at 1035.2 and 975.6 cm^{-1} was assigned to vibration of the interfacial O–H group on metal oxides [49, 50]. Moreover, the appearance of two weak peaks at 556.4 and 478.4 cm^{-1} was ascribed to stretching vibrations of the Mn–O and Fe–O bond, respectively, which indicated that the precipitates consisted of manganese oxides and iron oxides [51, 52].

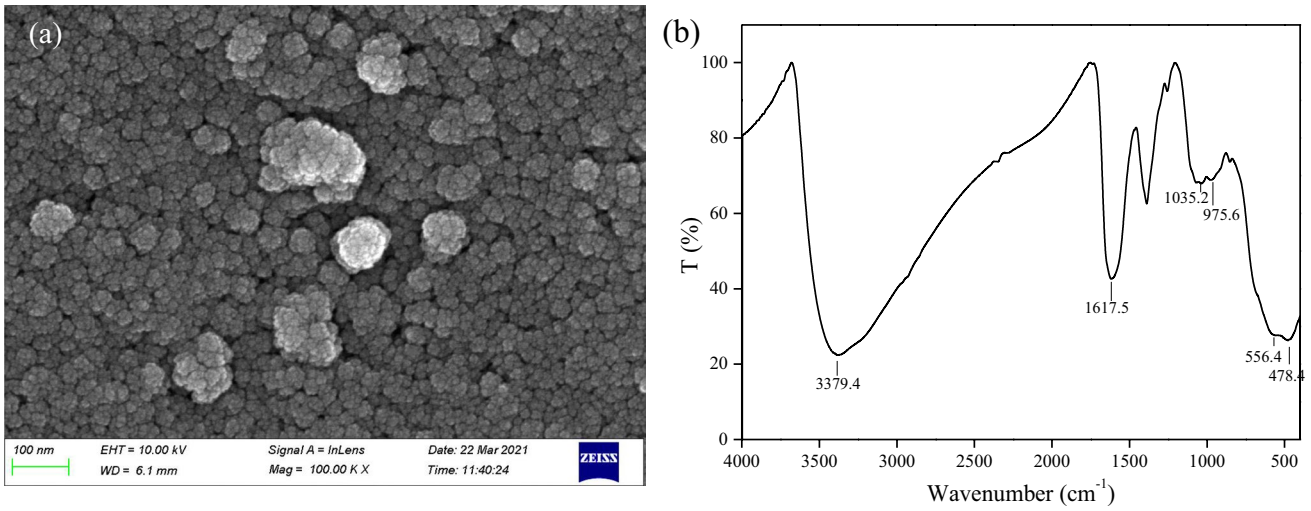

Fig. 4 **a** SEM image and **b** FTIR spectra of bio-generated sediment

The material composition of the sample was further revealed by the XPS analysis. Figure 5a presents the whole region scan of the sample. It showed that the principal elements were O, P, C, Fe, N, and Mn. The presence of C and N resulted from microorganisms. Peaks of Fe, Mn, and O illustrated the generation of iron and manganese oxides. Detailed XPS surveys on the region of O 1 s, Mn 2p, and Fe 2p are presented in Fig. 5b–d. As shown in Fig. 5b, the curve fitting of O1s spectra shows two different peaks. A peak located at 530.2 eV was associated with the Me-O band [53], and the other peak at 531.7 eV corresponded to Me-O–H hydroxyl groups that appeared due to metallic oxide [54, 55]. The photoelectron peaks for Mn 2p3/2 and 2p1/2 in Fig. 5c center at 641.65 and 653.35 eV, respectively. The peak of Mn 2p3/2 in the spectrum was not symmetrical, suggesting there may be more than one valence state of Mn. Then, the curve fitting of the Mn 2p3/2 spectra showed two peaks at approximately 641.1 eV and 642.6 eV, which could be assigned to Mn(III) in MnOOH and Mn(IV) in MnO_2, respectively [50, 56]. Moreover, the relative abundance of Mn(III) and Mn(IV) in the product was about 36.9% and 63.1%, respectively. The two valence states were normalized to an Mn average oxidation state of 3.63, which fell within the reported range [15, 56, 57]. As shown in Fig. 5d, the high-resolution Fe 2p XPS spectrum of the sample exhibited a binding energy peak at 711.4 eV (Fe 2p3/2) and a peak at 724.8 eV (Fe 2p 1/2) along with a satellite peak at 719.1 eV, which were indicative of Fe(III) species in FeOOH [50, 58].

N_2 adsorption–desorption isotherm was employed to investigate the specific surface area and pore characteristics of the sample, and the results are shown in Fig. 6. According to the International Union of Pure and Applied Chemistry (IUPAC), the adsorption–desorption curve showed classified type I isotherms with H4 type hysteresis loop as a result of capillary condensation, indicating the existence of micropores and mesopores [59, 60]. Based on the Barret-Joyner-Halenda (BJH) analysis, the pore size distribution was obtained. It can be seen that the continuous pore distribution of the sample narrowed, with the major distributions in the size range of < 2 nm. BET surface area, average pore size, and pore volume were calculated to be 329.335 m^2/g, 1.190 nm, and 0.162 cm^3/g, respectively.

In short, SEM, FTIR, and XPS analysis confirmed that the sediment was actually a mixture of poorly crystallized MnOOH, MnO_2, and FeOOH. While, as a common iron and nitrogen source for MnOB, ammonium ferric citrate in the inoculated JFM medium can be oxidized and precipitated as iron oxides [61]. More importantly, the BET specific surface area of the mixed oxides was significantly larger than that of biogenic manganese oxides and iron oxides reported in other studies [20, 25, 62, 63].

3.5 Kinetic analysis of Mn(II) oxidation by *Klebsiella* sp. strain M3 in acidic solution

In order to further understand the Mn(II) removal process, theory kinetics fitting was carried out. Pseudo-first-order kinetics was commonly used to represent the biological reaction, such as microbial Mn transformations (either oxidation or reduction), biodegradation of chlortetracycline via a microalgae-bacteria consortium, and biodegradation of bisphenol A by immobilized *Phanerochaete chrysosporium* beads [64–66]. The previous experiments in the study indicated that Mn(II) was removed from the water and completely bio-oxidized to Mn(III, IV), and abiotic Mn(II) oxidation almost did not happen. Based on the premise that bacteria was sufficient and the oxidation was only dependent on the Mn(II) content, the bio-oxidation of Mn(II) was

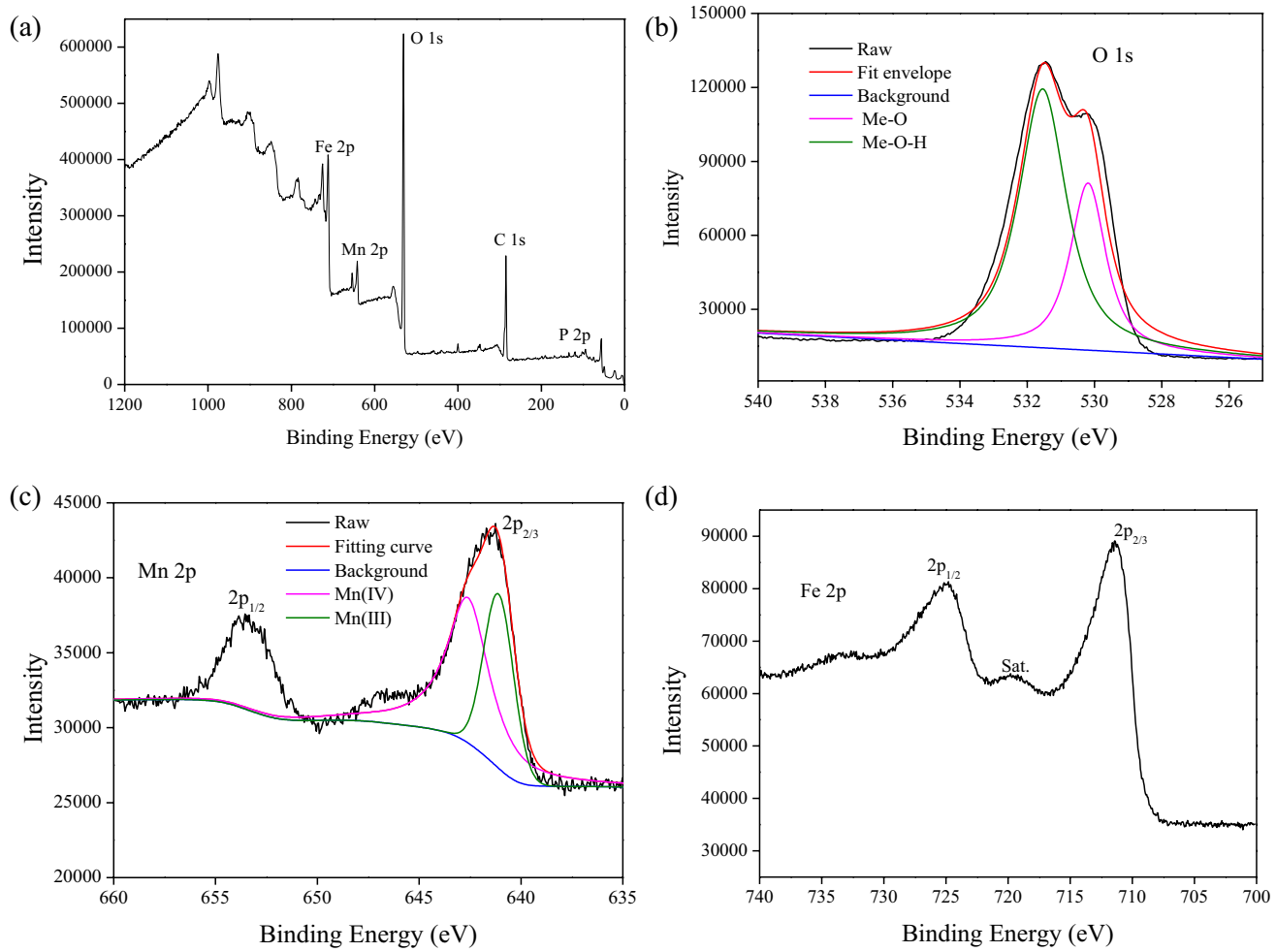

Fig. 5 **a** XPS wide survey of Mn-contained sediment and the high-resolution XPS survey of **b** O 1 s, **c** Mn 2p, and **d** Fe 2p

assumed to conform to the pseudo-first-order kinetic equation [67], which was expressed as Eq. (2).

$$\frac{d[Mn^{2+}]_t}{dt} = k_1[Mn^{2+}]t \quad (2)$$

After separation of variables and integration, it became:

$$ln\frac{[Mn^{2+}]_t}{[Mn^{2+}]_0} = -k_1 t \quad (3)$$

where k_1 is the first-order kinetic constant (h^{-1}), the meaning of $[Mn^{2+}]_0$ and $[Mn^{2+}]_t$ was the same as that in Eq. (1), and t is reaction time.

The kinetics of microbial Mn(II) oxidation in water as the pH ranged from 3.0 to 7.0 was evaluated. Moreover, the data from the earlier and middle stages of Mn removal curves were used for kinetic analysis, and points after 120 h were excluded. The fitting of pseudo-first-order for Mn(II) removal by *Klebsiella* sp. strain M3 is shown in Fig. 7. Calculated rate constants (k_1) and regression

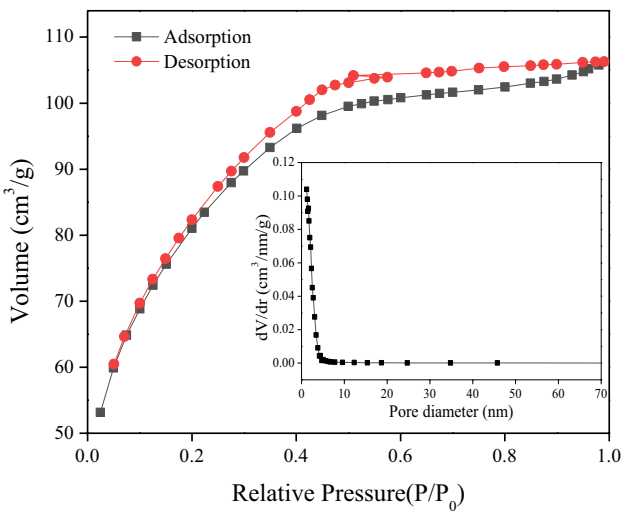

Fig. 6 Nitrogen adsorption/desorption isotherms and BJH pore size distribution (inset) of the sample

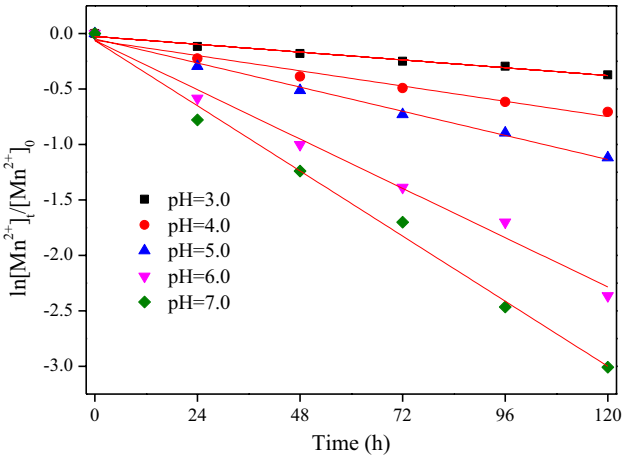

Fig. 7 The fitting curve of a pseudo-first-order kinetic model for Mn(II) removal by strain M3 under different solution pH

correlation coefficients (R^2) are summarized in Table S3. It was evident that microbial Mn(II) oxidation in acidic water followed the pseudo-first-order kinetic model. The rate constants obtained for Mn(II) removal ranged from 0.003 to 0.024 h^{-1}, and it was seriously reduced with the decrease of pH value. Cerrato et al. [64] isolated two strains of Mn(II)-oxidizing bacteria from the sedimentation basin of the water system, which were identified as *Bacillus cereus* and *Bacillus pumilus*. The pseudo-first-order rate constants for Mn-oxidation by these selected isolates with aeration air flushing under neutral conditions ranged from 0.106 to 0.659 $days^{-1}$. It was found that the obtained kinetic constant under acidic solution in our study was comparable to that of reported individual isolates under neutral conditions, implying the strong oxidation activity of isolated *Klebsiella* sp. strain M3.

3.6 Removal of Sb(III) from water during Mn(II) bio-mineralization process

3.6.1 Sb removal performance under different Mn(II) concentration

Many studies suggested that biogenic or chemical-prepared manganese oxides had adsorption ability towards Sb, Cd, and Pb [20, 22, 32, 49]. But up to now, the removal ability of in situ formed biogenic manganese oxides towards concomitant heavy metals in acidic wastewater was rarely investigated. After inoculation of strain M3, Sb concentration in the mixed solution at the initial pH of 6.0 was monitored, and the results are demonstrated in Fig. 8a. As Mn(II) concentration was 0, 10, 20, 30, 40, and 50 mg/L, residual Sb in water after 120 h of reaction was 8.20, 3.99, 3.27, 2.85, 2.25, and 3.03 mg/L, respectively. It showed that 18% of Sb(III) was removed, even though there was no Mn(II) in the solution. The removal of Sb was probably caused by the generation of a certain amount of manganese oxides in 10 mL of inoculated bacteria. Furthermore, more Sb(III) was obviously removed from the water as the initial Mn(II) concentration increased from 10 to 40 mg/L, but the trend marked a reversal when Mn(II) level reached 50 mg/L. This was probably because the toxicities of a high Mn(II) level and Sb(III) would be largely exacerbated and thus suppressed the oxidation ability of *Klebsiella* sp. strain M3 [68].

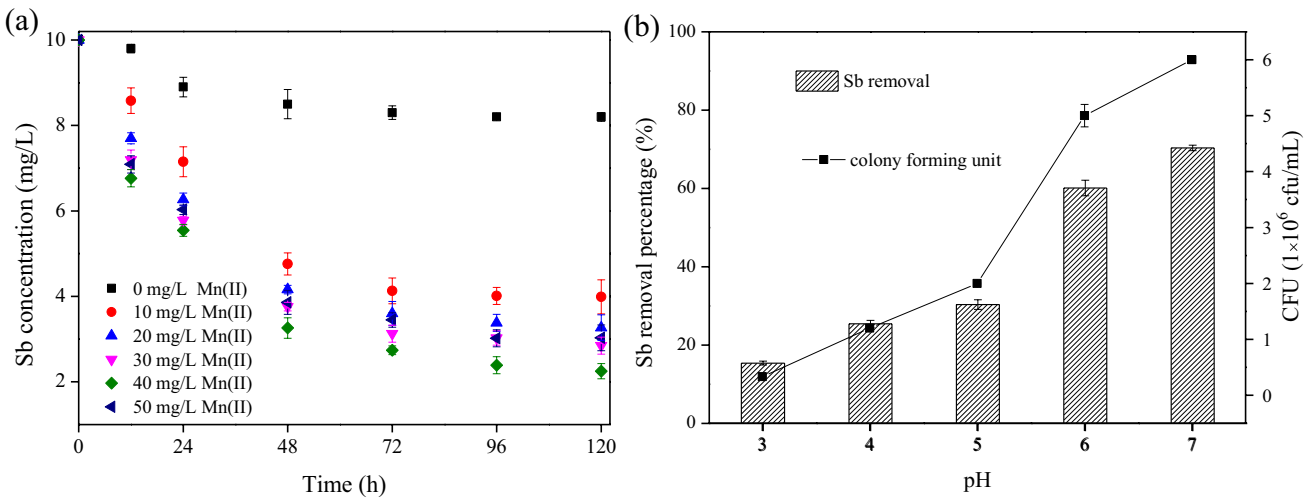

Fig. 8 **a** Sb concentration changed along with microbial oxidation of Mn(II) and **b** the final Sb removal rate and bacteria biomass

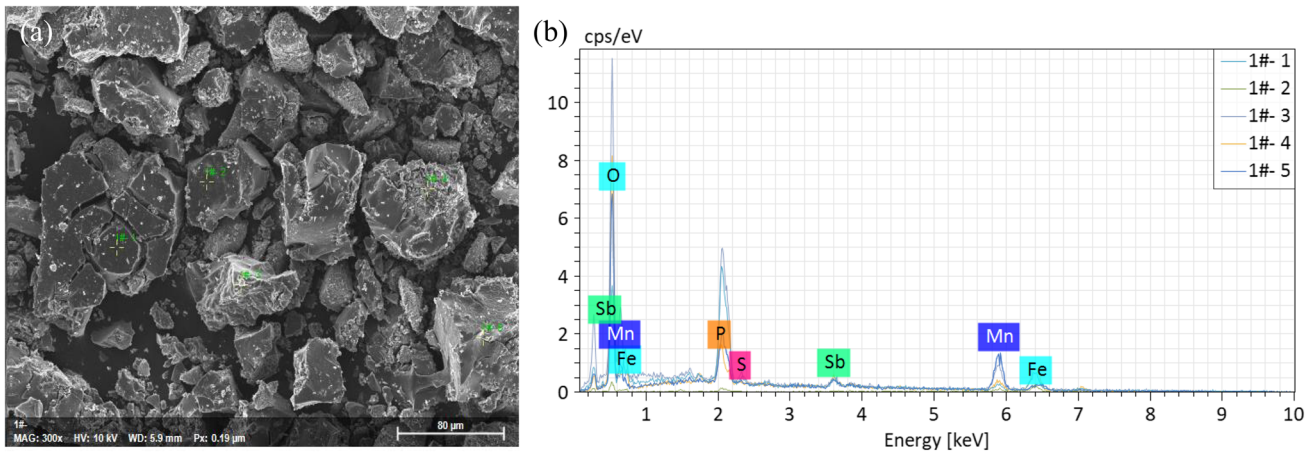

Fig. 9 **a** SEM image and **b** EDX patterns of the Sb-contained product

3.6.2 Sb removal performance under different solutions pH

As can be seen from Fig. 8b, when initial solution pH was 3.0, 4.0, 5.0, 6.0, and 7.0, the final Sb(III) removal rates during the bio-mineralization of Mn(II) are 15.4%, 25.4%, 30.3%, 60.1%, and 70.4%, respectively. Meanwhile, the colony numbers of strain M3 in solution were 3.3×10^5, 1.2×10^6, 2.0×10^6, 5.0×10^6, and 6.0×10^6 CFU/mL, respectively. It can be seen that Sb(III) removal and bacteria growth in acidic solution were worse than that in the neutral condition. It was known that the oxidation capacity of *Klebsiella* sp. strain M3 became weak in acidic conditions. These indicated that the decrease of Sb(III) removal may be closely related to the activity of the strain.

The data in the batch experiments showed that the Sb(III) removal ability of BMO under pH 3.0–7.0, expressed as Sb/Mn mass ratio, varied from about 0.15 to 0.7. Bai et al. also investigated the removal of 1.21 mg/L Sb(III) by in situ BMO formed by *Pseudomonas* sp. QJX-1 in the neutral medium containing 5 mg/L Mn(II) [30]. Although desorption occurred concurrently with adsorption, 44.38% of Sb was removed after 132 h, corresponding to a removal capacity of 0.15 mg total Sb/mg total Mn. So, the formed BMO in the present study possessed a high binding capacity with associated metal Sb, which proved that *Klebsiella* sp. strain M3 had great potential to oxidize Mn(II) and remove associated Sb(III) in acid mine drainage.

3.6.3 Sb removal mechanism

SEM–EDX, FTIR, and XPS analysis of product collected from Sb immobilization were conducted at the end of the experiment. As shown in Fig. 9a, the product was micron-sized substances with irregularly shaped blocks. Moreover, the high-resolution SEM image (Fig. S5) shows that these aggregates were composed of uniform nanoparticles, which was similar to the morphology of biogenic metal oxides as demonstrated in Fig. 4a.

EDX analysis was conducted on five different parts of the sample (Fig. 9b). As shown in Table 1, elements O, Mn, Fe, Sb, P, and S are mainly present on the surface of the product. The occurrence of S and P was due to the bacteria. The presence of Fe, Mn, and O proved the generation of manganese oxides and iron oxides as mentioned in Sect. 3.4. However, the constituent ratio of Fe and Mn in the five parts was not the same. This demonstrated that it was not made up of ferromanganese oxides, but an ordinary mixture of iron oxides and manganese oxides. More importantly, the presence of Sb in the sample indicated that Sb(III) in the solution was transferred to the surface of the precipitates along with the microbial Mn(II) oxidation.

The FTIR spectrum of the Sb-contained product is shown in Fig. 10a. It was obvious that after Sb(III) removal reaction, the peak at 1035.2 and 975 cm^{-1} (Fig. 4b) gradually shifted to 1070.5 and 953.6 cm^{-1}, indicating that the O–H

Table 1 The ratio of elements on the surface of the reaction product

Sample	O	P	S	Mn	Fe	Sb	Total
1#-1	11.70	15.29	0.68	10.82	55.24	6.28	100.01
1#-2	4.68	1.26	0.23	18.20	73.54	2.09	100
1#-3	26.85	13.51	1.11	43.41	7.68	7.44	100
1#-4	18.74	4.73	0.20	12.95	55.88	7.49	99.99
1#-5	16.60	5.92	0.34	61.91	9.12	6.10	99.99

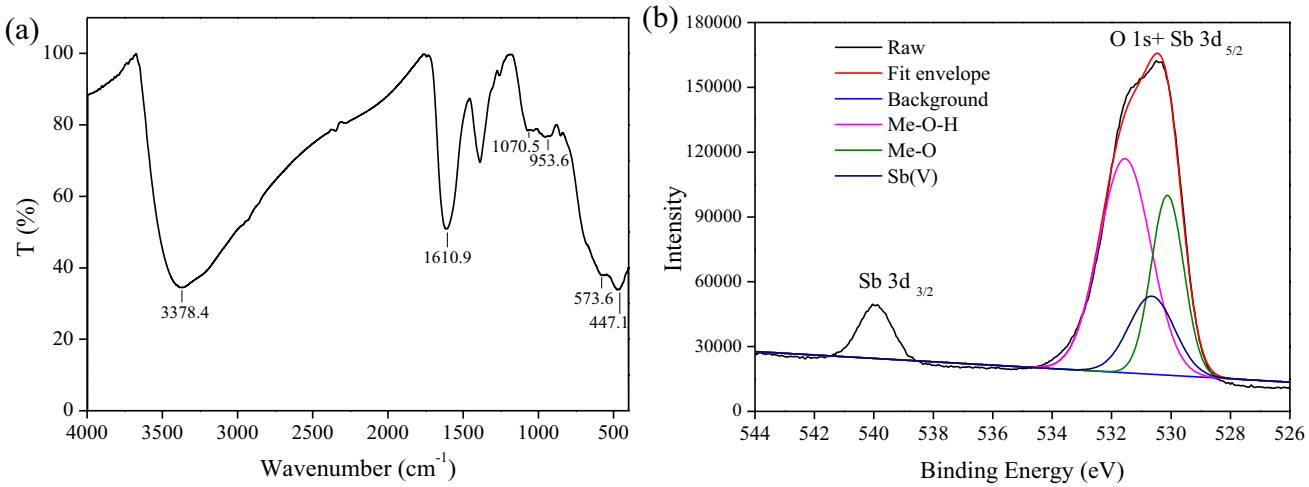

Fig. 10 **a** FITR spectrum for Sb-contained precipitate and **b** high-resolution XPS survey of O 1 s + Sb 3d

bond had interacted with Sb. At the same time, the peak at 556.4 and 478.4 cm^{-1} as a result of stretching vibrations of Mn–O and Fe–O bond shifted after the removal of Sb. Xu et al. [69] also illustrated the FTIR spectra of the chemical prepared MnO_2 before and after adsorbing Sb(III); however, there were no obvious peaks for sample MnO_2–Sb, indicating the weak binding of Sb to Mn oxide.

The electronic structures and the interactions between Sb(III) and the biogenetic metal oxides were further revealed by the XPS analysis. As shown in Fig. S6, the principal elements at the product surface are O, Sb, C, N, P, Fe, and Mn, which was in agreement with EDX analysis. A detailed XPS survey on the region of O 1 s and Sb 3d is presented in Fig. 10b. The particles exhibited Sb 3d $_{3/2}$ binding energy of about 540 eV, which indicated the presence of Sb species [70]. There was some overlap between the photoelectron peaks of Sb 3d $_{5/2}$ and O 1 s, but the curve fitting of O 1 s and Sb 3d $_{5/2}$ spectra showed three different peaks at approximately 531.7 eV, 530.6 eV, and 530.2 eV. According to the XPS analysis in Sect. 3.4, the two peaks at 531.7 and 530.2 eV were assigned to Me-O–H and Me-O bands, and the peak at about 530.6 eV was assigned to Sb(V)[71]. It indicated that Sb(III) in acidic water was oxidized to Sb(V) as the progress of Mn(II) oxidation.

It has been reported that the Sb(III) can be easily oxidized by manganese oxides, but hard to be oxidized by iron oxides [31, 49, 72]. Some studies also revealed that the Mn oxidized mineral was an efficient heavy metal scavenger. For example, trace cadmium in irrigation water was scavenged and immobilized in the crystal lattice of porous spongy-like birnessite which was generated due to oxidation of Mn ion by *Bacillus* in biological soil crust [73]. Wang et al. found that during adsorptive removal of Sb(III) from water by exogenous BMO, approximately 20% of produced Sb(V) may incorporate into the octahedral layers to form stable Mn–O-$Sb(OH)_5^-$ [74]. Based on the SEM–EDX, FTIR, and XPS analysis in the study, it was reasonably inferred that along with the progress of microbial Mn(II) oxidation, concomitant Sb(III) can be removed from acidic wastewater and immobilized in precipitates.

4 Conclusions

To treat the acid mine drainage, a new strain of MnOB with high tolerance towards Mn(II) in acidic solution was isolated from activated sludge in a sewage treatment plant. Phylogenetic analysis showed that the strain belonged to the *Klebsiella* genus. Although the optimal pH for cultivation and oxidation ability of the strain was 7.0, it can grow in water with initial pH of 3.0, and 36% of 10 mg/L Mn(II) was removed with inoculation of 2%. Characterization of SEM, XRD, FTIR, XPS, and N_2 adsorption–desorption isotherm showed that biogenic precipitates were composed of poorly crystallized spherical nanoparticles with high BET surface area. Moreover, it was a mixture of amorphous FeOOH, MnOOH, and MnO_2, and the average Mn oxidation number of manganese oxides was about 3.63. Microbial Mn(II) oxidation followed the pseudo-first-order kinetic model under acidic conditions, and the rate constants ranged from 0.003 to 0.024 h^{-1}. More importantly, along with the progress of Mn(II) bio-oxidation, the coexisting Sb(III) was removed from the water and immobilized in precipitates.

Supplementary Information The online version contains supplementary material available at https://doi.org/10.1007/s13399-022-03376-2.

Author contribution Yongchao Li: Conceptualization, supervision, reviewing, and editing, funding. Jialing Liu: Software, investigation, writing-original draft, resources. Zhonggeng Mo: Project administration, visualization, acquisition. Zheng Xu: Methodology, formal analysis, investigation.

Funding This work is financially sponsored by the National Natural Science Foundation of China (No. 42177380 and 51504094).

Data availability All data generated or analyzed during this study are included in this published article [and its supplementary information files].

Declarations

Ethics approval The manuscript does not include any experiments which were carried out with human volunteers or any kind of animals.

Competing interests The authors declare no competing interests.

References

1. Röllin HB, Nogueira C (2011) Manganese: environmental pollution and health effects. Encycl Environ Health 617–629.
2. Gerke TL, Little BJ, Maynard JB (2016) Manganese deposition in drinking water distribution systems. Sci Total Environ 541:184–193
3. Council E (1998) Council directive 98/83 about water quality intended for human consumption. Off J Eur Communities L 330:32–54
4. United States Environmental Protection Agency (2013) Secondary drinking water regulations: guidance for nuisance chemicals, USEPA: Washington. DC, USA
5. Xiang J, Chen J, Bagas L, Li S, Wei H, Chen B (2020) Southern China's manganese resource assessment: an overview of resource status, mineral system, and prediction model. Ore Geol Rev 116:103261
6. Pharoe BK, Evdokimov AN, Bushuyev YY (2020) Mineral composition and reconstruction of the source areas of manganese-bearing alluvial deposits in the Ventersdorp area. South Africa J Afr Earth Sci 168:10384
7. Queiroz HM, Ying SC, Abernathy M, Barcellos D, Gabriel FA, Otero XL, Nóbrega GN, Bernardino AF, Ferreira TO (2021) Manganese: the overlooked contaminant in the world largest mine tailings dam collapse. Environ Int 146:106284
8. Calugarua IL, Genty T, Neculita CM (2021) Treatment of manganese, in the presence or absence of iron, in acid and neutral mine drainage using raw vs half-calcined dolomite. Miner Eng 160:106666
9. Li Y, Xu Z, Ma H, Hursthouse AS (2019) Removal of manganese(II) from acid mine wastewater: a review of the challenges and opportunities with special emphasis on Mn-oxidizing bacteria and microalgae. Water 11:2493
10. Torres E, Lozano A, Macías F, Gomez-Arias A, Castillo J, Ayora C (2018) Passive elimination of sulfate and metals from acid mine drainage using combined limestone and barium carbonate systems. J Clean Prod 182:114–123
11. Patil DS, Chavan SM, Oubagaranadin JUK (2016) A review of technologies for manganese removal from wastewaters. J Environ Chem Eng 4:468–487
12. Baltrėnaitė-Gedienė E, Leonavičienė T, Baltrėnas P (2020) Comparison of CU(II), MN(II) and ZN(II) adsorption on biochar using diagnostic and simulation models. Chemosphere 245:125562
13. Lan S, Qin Z, Wang X, Yan Y, Tang Y, Feng X, Zhang Q (2021) Kinetics of Mn(II) adsorption and catalytic oxidation on the surface of ferrihydrite. Sci Total Environ 791:148225
14. Strauss ML, Diaz LA, McNally J, Klaehn J, Lister TE (2021) Separation of cobalt, nickel, and manganese in leach solutions of waste lithium-ion batteries using Dowex M4195 ion exchange resin. Hydrometallurgy 206:105757
15. Li H, Tang Y, Wu Y, Wang Y, Huang H, Huang Y, Liang F, Qin T (2021) Bio-immobilization of soluble Mn(II) in aqueous solution with co-occurred Mn(II)-oxidizing bacteria: facilitation or inhibition? J Environ Chem Eng 9:106448
16. Shoiful A, Ohta T, Kambara H, Matsushita S, Kindaichi T, Ozaki N, Aoi Y, Imachi H, Ohashi A (2020) Multiple organic substrates support Mn(II) removal with enrichment of Mn(II)-oxidizing bacteria. J Environ Manage 259:109771
17. Marsidi N, Hasan HA, Abdullah SRS (2018) A review of biological aerated filters for iron and manganese ions removal in water treatment. J Water Process Eng 2:1–12
18. Wang M, Xu Z, Dong B, Zeng Y, Chen S, Zhang Y, Huang Y, Pei X (2022) An efficient manganese-oxidizing fungus *Cladosporium halotolerans* strain XM01: Mn(II) oxidization and Cd adsorption behavior. Chemosphere 287:132026
19. Chen L, Zhang X, Zhang M, Zhu Y, Zhuo R (2022) Removal of heavy-metal pollutants by white rot fungi: mechanisms, achievements, and perspectives. J Clean Prod 354:131681
20. Zhou D, Kim DG, Ko SO (2015) Heavy metal adsorption with biogenic manganese oxides generated by *Pseudomonas putida* strain MnB1. J Ind Eng Chem 24:132–139
21. Toyoda K, Tebo BM (2013) The effect of Ca^{2+} ions and ionic strength on Mn(II) oxidation by spores of the marine *Bacillus* sp. SG-1. Geochim Cosmochim Acta 101:1–11
22. Wan W, Xing Y, Qin X, Li X, Liu S, Luo X, Huang Q, Chen W (2020) A manganese-oxidizing bacterial consortium and its biogenic Mn oxides for dye decolorization and heavy metal adsorption. Chemosphere 253:126627
23. Miyata N, Tani Y, Sakata M, Iwahori K (2007) Microbial manganese oxide formation and interaction with toxic metal ions. J Biosci Bioeng 104:1–8
24. Su J, Deng L, Huang L, Guo S, Liu F, He J (2014) Catalytic oxidation of manganese(II) by multicopper oxidase *CueO* and characterization of the biogenic Mn oxide. Water Res 56:304–313
25. Zheng J (2013) Mn^{2+} Oxidization by a manganese-oxidizing bacterium and the characteristics and properties of its products. Master's Thesis, Huazhong Agriculture University, Wuhan, China.
26. Chen G, Jiang CL, Liu RL, Xie ZM, Liu ZH, Cen SD, Tao CY, Guo SH (2021) Leaching kinetics of manganese from pyrolusite using pyrite as a reductant under microwave heating. Sep Purif Technol 277:119472
27. Neculita CM, Rosa E (2019) A review of the implications and challenges of manganese removal from mine drainage. Chemosphere 214:491–510
28. Outram JG, Couperthwaite SJ, Millar GJ (2018) Enhanced removal of high Mn(II) and minor heavy metals from acid mine drainage using tunnelled manganese oxides. J Environ Chem Eng 6:3249–3261
29. Boyle RW, Jonasson IR (1984) The geochemistry of antimony and its use as an indicator element in geochemical prospecting. J Geochem Explor 20:223–302
30. Bai Y, Chang Y, Liang J, Chen C, Qu J (2016) Treatment of groundwater containing Mn(II), Fe(II), As(III) and Sb(III) by bioaugmented quartz-sand filters. Water Res 106:126–134
31. Wang Y, Tsang YF, Wang H, Sun Y, Song Y, Pan X, Luo S (2020) Effective stabilization of arsenic in contaminated soils with biogenic manganese oxide (BMO) materials. Environ Pollut 258:113481

32. Holguera JG, Etui ID, Jensen LHS, Peña J (2018) Contaminant loading and competitive access of Pb, Zn and Mn(III) to vacancy sites in biogenic MnO_2. Chem Geol 502:76–87
33. Zhang Y, Tang Y, Qin Z, Luo P, Ma Z, Tan M, Kang H, Huang Z (2019) A novel manganese oxidizing bacterium-*Aeromonas hydrophila* strain DS02: Mn(II) oxidization and biogenic Mn oxides generation. J Hazard Mater 367:539–545
34. Weisburg WG, Barns SM, Pelletier DA, Lane DJ (1991) 16S ribosomal DNA amplification for phylogenetic study. J Bacteriol 173:697–703
35. Fujinami W, Nishikawa K, Ozawa S, Hasegawa Y, Takebe J (2021) Correlation between the relative abundance of oral bacteria and *Candida albicans* in denture and dental plaques. J Oral Biosci 63:175–183
36. Ghaedi M, Montazerozohori M, Sajedi M, Roosta M, Nickoosiar Jahromi M, Asghari A (2013) Comparison of novel sorbents for preconcentration of metal ions prior to their flame atomic absorption spectrometry determination. J Ind Eng Chem 19:1781–1787
37. Schug AR, Bartel A, Meurer M, Scholtzek AD, Brombach J, Hensel V, Fanning S, Schwarz S, Fessler AT (2020) Comparison of two methods for cell count determination in the course of biocide susceptibility testing. Vet Microbiol 251:108831
38. Kruger MC, Bertin PN, Heipieper HJ, Arsene-Ploetze F (2013) Bacterial metabolism of environmental arsenic-mechanisms and biotechnological applications. Appl Microbiol Biot 97:3827–3841
39. Nies DH (1999) Microbial heavy-metal resistance. Appl Microbiol Biot 51:730–750
40 Das R, Liang Z, Li G, An T (2020) A non-blue laccase of Bacillus sp GZB displays manganese-oxidase activity: a study of laccase characterization, Mn(II) oxidation and prediction of Mn(II) oxidation mechanism. Chemosphere 252:126619
41. Ren HT, Jia SY, Wu SH, Liu Y, Hua C, Han X (2013) Abiotic oxidation of Mn(II) induced oxidation and mobilization of As(III) in the presence of magnetite and hematite. J Hazard Mater 254–255:89–97
42. Gauvry E, Mathot AG, Couvert O, Leguérinel I, Coroller L (2021) Effects of temperature, pH and water activity on the growth and the sporulation abilities of *Bacillus subtilis* BSB1. Int J Food Microbiol 337:108915
43. Kikot P, Viera M, Mignone C, Donati E (2010) Study of the effect of pH and dissolved heavy metals on the growth of sulfate-reducing bacteria by a fractional factorial design. Hydrometallurgy 104:494–500
44. Zhang J, Lion LW, Nelson YM, Shuler ML, Ghiorse W (2002) Kinetics of Mn(II) oxidation by *Leptothrix discophora* SS1. Geochim Cosmochim Acta 66:773–781
45 Yin Z, Xia D, Shen M, Zhu D, Cai H, Wu M, Zhu Q, Kang Y (2020) Tetracycline degradation by Klebsiella sp strain TR5: proposed degradation pathway and possible genes involved. Chemosphere 253:126729
46. Liu T, Li X, Li F, Zhang W, Chen M, Zhou S. Reduction of iron oxides by *Klebsiella pneumoniae* L17: kinetics and surface properties. Colloid Surface A 379:143–150.
47. Mandernack KW, Post J, Tebo BM (1995) Manganese mineral formation by bacterial spores of the marine *Bacillus*, strain SG-1: evidence for the direct oxidation of Mn(II) to Mn(IV). Geochim Cosmochim Acta 59:4393–4408
48. Ye J, Cong X, Zhang P, Zeng G, Hoffmann E, Liu Y, Wu Y, Zhang H, Fang W, Hahn HH (2016) Application of acid-activated Bauxsol for wastewater treatment with high phosphate concentration: characterization, adsorption optimization, and desorption behaviors. J Environ Manage 167:1–7
49. Wang X, Yang Y, Tao L, He M (2021) Antimonite oxidation and adsorption onto two tunnel-structured manganese oxides: Implications for antimony mobility. Chem Geol 579:120336
50. Xu R, Li Q, Nan X, Jiang G, Wang L, Xiong J, Yang Y, Xu B, Jiang T (2022) Simultaneous removal of antimony(III/V) and arsenic(III/V) from aqueous solution by bacteria–mediated kaolin@Fe–Mn binary (hydr) oxides composites. Appl Clay Sci 217:106392
51. Yuan A, Zhang Q (2006) A novel hybrid manganese dioxide/activated carbon supercapacitor using lithium hydroxide electrolyte. Electrochem Commun 8:1173–1178
52. Miller AZ, Dionísio A, Sequeira Braga MA, Hernández-Mariné M, Afonso MJ, Muralha VSF, Herrera LK, Raabe J, Fernandez-Cortes A, Cuezva S, Hermosin B, Sanchez-Moral S, Chaminé H, Saiz-Jimenez C (2012) Biogenic Mn oxide minerals coating in a subsurface granite environment. Chem Geol 322–323:181–191
53. Iatsunskyi I, Kempiński M, Jancelewicz M, Załęskia K, Jurga S, Smyntyna V (2015) Structural and XPS characterization of ALD Al_2O_3 coated porous silicon. Vacuum 113:52–58
54. Deliyanni EA, Nalbandian L, Matis KA (2006) Adsorptive removal of arsenites by a nanocrystalline hybrid surfactant–akaganeite sorbent. J Colloid Interface Sci 302:458–466
55. Chenakin S, Kruse N (2020) XPS characterization of transition metal oxalates. Appl Surf Sci 515:146041
56. Tu J, Yang Z, Hu C, Qu J (2014) Characterization and reactivity of biogenic manganese oxides for ciprofloxacin oxidation. J Environ Sci 26:1154–1161
57. Zheng Q, Tu S, Hou J, Ni C, Wang M, Ren L, Wang M, Cao M, Xiong S, Tan W (2021) Insights into the underlying mechanisms of stability working for As(III) removal by Fe-Mn binary oxide as a highly efficient adsorbent. Water Res 203:117558
58. Wu P, Zhou C, Li Y, Zhang M, Tao P, Liu Q, Cui W (2021) Flower-like FeOOH hybridized with carbon quantum dots for efficient photo-Fenton degradation of organic pollutants. Appl Surf Sci 540:148362
59. Sing KS (1985) Reporting physisorption data for gas/solid systems with special reference to the determination of surface area and porosity (Recommendations 1984). Pure Appl Chem 57:603–619
60. Thommes M, Kaneko K, Neimark AV, Olivier JP, Rodriguez-Reinoso F, Rouquerol J, Sing KSW (2015) Physisorption of gases, with special reference to the evaluation of surface area and pore size distribution (IUPAC Technical Report). Pure Appl Chem 87:1051–1069
61. Li Y, Liu J, Mo Z, Li L (2022) Influence of different iron sources on Sb(III) removal from water by active iron-oxidizing bacteria and its mechanism. Water Sci Technol 85:1412
62. Hu Y, Chen X, Liu Z, Wang G, Liao S (2016) Activated carbon doped with biogenic manganese oxides for the removal of indigo carmine. J Environ Manage 166:512–518
63. Căpraru A, Moacă EA, Păcurariu C, Ianoş R, Lazău R, Barbu-Tudoran L (2021) Development and characterization of magnetic iron oxide nanoparticles using microwave for the combustion reaction ignition, as possible candidates for biomedical applications. Powder Technol 394:1026–1038
64. Cerrato JM, Falkinham JO, Dietrich AM, Knocke WR, McKinney CW, Pruden A (2010) Manganese-oxidizing and -reducing microorganisms isolated from biofilms in chlorinated drinking water systems. Water Res 44:3935–3945
65. Wang Y, He Y, Li X, Nagarajan D, Chang JS (2022) Enhanced biodegradation of chlortetracycline via a microalgae-bacteria consortium. Bioresource Technol 343:126149
66. Wang J, Xie Y, Hou J, Zhou X, Chen J, Yao C, Zhang Y, Li Y (2022) Biodegradation of bisphenol A by alginate immobilized *Phanerochaete chrysosporium* beads: continuous cyclic treatment and degradation pathway analysis. Biochem Eng J 177:108212
67. Wang M, Xu Z, Dong B, Zeng Y, Chen S, Zhang Y, Huang Y, Pei X (2022) An efficient manganese-oxidizing fungus *Cladosporium*

halotolerans strain XM01: Mn(II) oxidization and Cd adsorption behavior. Chemosphere 287:132026
68. Cao Q, Liu W, Gu Y, Xie L, Jiang W, Gao Y, Yang L (2020) Synergetic enhancement toxicity of copper, cadmium and microcystin-LR to the *Ceratophyllum demersum* L. Toxicon 186:151–159
69. Xu W, Wang H, Liu R, Zhao X, Qu J (2011) The mechanism of antimony(III) removal and its reactions on the surfaces of Fe–Mn binary oxide. J Colloid Interf Sci 363:320–326
70. Stamenković T, Bundaleski N, Barudžija T, Validžić I, Lojpur V (2021) XPS study of iodine and tin doped Sb_2S_3 nanostructures affected by non-uniform charging. Appl Surf Sci 567:150822
71. Li Y, Xu Z, Wu J, Mo P (2020) Efficiency and mechanisms of antimony removal from wastewater using mixed cultures of iron-oxidizing bacteria and sulfate-reducing bacteria based on scrap iron. Sep Purif Technol 246:116756
72. Zhang C, He M, Lin C, Ouyang W, Liu X (2022) Oxidation and adsorption of Sb(III) in the presence of iron (hydr)oxides and dissolved Mn(II). Chem Geol 591:120725
73. Peng L, Deng X, Song H, Tan X, Gu J, Luo S, Lei M (2019) Manganese enhances the immobilization of trace cadmium from irrigation water in biological soil crust. Ecotox Environ Safe 168:369–377
74. Wang H, Lv Z, Song Y, Wang Y, Zhang D, Sun Y, Tsang YF, Pan X (2019) Adsorptive removal of Sb(III) from wastewater by environmentally-friendly biogenic manganese oxide (BMO) materials: efficiency and mechanisms. Process Saf Environ 124:223–230